Synthesis and Characterization of ABA Triblock Copolymers Containing Smectic C* Liquid Crystal Side Chains via Ring-Opening Metathesis Polymerization Using a Bimetallic Molybdenum Initiator

Andrea J. Gabert,[†] Eric Verploegen,[‡] Paula T. Hammond,*[,§] and Richard R. Schrock*[,†]

Department of Chemistry, Rm 6-331, Department of Materials Science and Engineering, and Department of Chemical Engineering, Rm 66-550, Massachusetts Institute of Technology, 77 Massachusetts Avenue, Cambridge, Massachusetts 02139

Received January 31, 2006; Revised Manuscript Received April 3, 2006

ABSTRACT: A series of monomers suitable for ring-opening metathesis polymerization (ROMP) containing a side chain liquid crystal mesogen have been synthesized, where the mesogen is biphenyl-4-carboxylic acid 4-(1-butoxycarbonyl-ethoxy)phenyl ester (abbreviated as **BPP4**). Two of the monomers have **BPP4** attached to norbornene with a 6- or 10-carbon spacer ((*R*)-4′-(5-bicyclo[2.2.1]hept-5-en-2-yl-pentyloxy)-BPP4, **NB6wBPP4**, and (*R*)-4′-(10-bicyclo[2.2.1]hept-5-en-2-yl-decyloxy)-BPP4, **NB10wBPP4**, respectively), and the third monomer has **BPP4** attached to norbornadiene via a 10-carbon spacer ((*R*)-4′-(10-bicyclo[2.2.1]hepta-2,5-dien-2-yl-decyloxy)-BPP4, **NBD10wBPP4**). The monomers were polymerized by ROMP using the bimetallic initiator, {Mo(NAr)-$(OR_{F6})_2$[=CHC_5H_4]}$_2$Fe (Ar = 2,6-diisopropylphenyl, OR_{F6} = $OCMe(CF_3)_2$). ABA triblock copolymers were also synthesized where the B = **NBD10wBPP4** or **NB*n*wBPP4** (n = 6, 10) and A = methyltetracyclododecene (MTD). All polymerizations are living with isolated yields greater than 90% and polydispersities ranging from less than 1.05 to 1.31. Polarized optical microscopy (POM) and differential scanning calorimetry (DSC) studies revealed glass transition temperatures for the inner block of the triblock copolymers at ∼20 °C and smectic-to-isotropic transitions around 150 °C. Small-angle X-ray scattering (SAXS) indicated that the triblock copolymers exhibit phase segregation. In addition, it was determined from SAXS data that the triblock copolymer containing **NB6wBPP4** forms smectic C* monolayers while the triblock copolymers that contain **NB10wBPP4** and **NBD10wBPP4** form smectic C* bilayers at room temperature. DMA of the triblock copolymers reveals an elastic plateau above the T_g of the center block, indicating these systems exhibit elastomeric behavior at elevated temperature and could form the basis of interesting materials for LC shape-memory elastomers.

Introduction

Living polymerization methods allow for the synthesis of polymers with well-defined structures and controlled chemical compositions as well as the formation of a wide range of block copolymers.[1−5] Under appropriate conditions and choice of monomer, block copolymers can self-assemble into various morphologies with nanometer-sized domains.[6] ABA triblock copolymers which exhibit microphase separation can act as thermoplastic elastomers (TPEs) when the outer block is amorphous and has a high glass transition temperature (T_g) and the inner block is flexible and has a low T_g.[7]

New classes of thermoplastic elastomers can arise when the central block is functionalized with liquid crystal mesogens, forming novel block copolymers referred to as thermoplastic liquid crystalline elastomers (TPLCE);[8−10] these materials allow the formation of uniformly oriented domains using thermoplastic processing methods, while utilizing the block copolymer interface as a means of further stabilizing or influencing the LC phase of interest existent within the soft, continuous phase. In general, liquid crystalline elastomers (LCEs) are of interest because they possess electromechanical and electrooptical properties that have the potential application for moderate to high strain actuating polymers. LCEs have also been known to exhibit the property of "soft elasticity",[11−14] a characteristic which makes them interesting energy absorbing or damping materials. Most LCEs that have been examined thus far have been covalently cross-linked siloxane-based materials that must be processed in a two-stage process to achieve orientation;[15−19] the processing advantages of thermoplastics are not accessible in such systems, and some limitations to extent of cross-linking exist due to the fact that cross-links can destabilize the LC phase.

Mesogens which exhibit the chiral smectic C* phase are of particular interest because this phase has been found to exhibit ferroelectric and piezoelectric properties. The block copolymer interface of TPLCEs, also known as the intermaterial dividing surface (IMDS), allows for the alignment of the liquid crystal mesogens, unlike homogeneous liquid crystal phases which require surface modification techniques for alignment. The IMDS also provides confinement within small gaps which has been found to unwind the pitch of the chiral smectic C* phase.[20] The interesting properties and potential applications of these polymers have been the focus of recent research by several groups, the polymers synthesized mainly by anionic polymerization of mesogen-functionalized monomers or by attachment of the mesogen to a preexisting functionalized block copolymer backbone.[10,16,21−30]

One living polymerization method that can be employed for the synthesis of well-defined triblock copolymers is ring-opening metathesis polymerization (ROMP).[5] Although monomers suitable for ROMP have been synthesized that contain liquid crystal mesogens,[31−35] no work has been completed with smectic C* mesogens. (Several reviews are available.[36−38]) In addition, despite examples of the synthesis of ABA triblock copolymers solely by ROMP,[39−43] there are no examples in which the central block is functionalized by liquid crystal mesogens. Therefore,

[†] Department of Chemistry.
[‡] Department of Materials Science and Engineering.
[§] Department of Chemical Engineering.
* Corresponding authors. E-mail: hammond@mit.edu, rrs@mit.edu.

10.1021/ma060243x CCC: $33.50
Published on Web 05/12/2006

there has been no examination of the potential for triblock copolymers synthesized via ROMP to function as TPLCEs. Triblock copolymers synthesized via ROMP should have predictable molecular weights, low polydispersities, tunable mesogen density, and well-defined polymer architectures.

We recently reported the synthesis of a series of bimetallic molybdenum initiators which are active for living ROMP.[41] These catalysts allow for the controlled synthesis of well-defined triblock copolymers. Bifunctional initiators have the benefit of allowing for the synthesis of symmetric triblock copolymers with two sequential additions of monomer, as opposed to the monofunctional catalysts which require three additions. In addition, use of a bifunctional initiator should eliminate any AB impurites that are found with other synthetic methods, and they may also allow access to ABA polymers that would otherwise be unavailable for investigation. We have expanded the use of the bimetallic molybdenum initiators for the synthesis of ABA triblock copolymers where the A block is composed of high-T_g amorphous methyltetracyclododecene (MTD) and the central block is functionalized by liquid crystal mesogens. Through examination of the thermal and mechanical properties of the synthesized polymers, we are beginning to explore the possibility of ROMP triblock copolymers that function as TPLCEs. Herein, we report the synthesis of a series of monomers suitable for ROMP which contain a smectic C* mesogen, **BPP4**[44] (biphenyl-4-carboxylic acid 4-(1-butoxycarbonylethoxy)phenyl ester), the synthesis of ABA triblock copolymers, and the thermal and mechanical characterization of the resulting polymers. These systems exhibit a rubbery plateau above room temperature; the ability to induce high levels of orientation in the continuous LC phase via stretching at high temperatures combined with the ability to quench the stretched orientation of the film at room temperature may lead to applications as high-temperature TPLCE actuators or as field-activated shape memory polymers.

Experimental Section

General Procedures. All manipulations were performed under nitrogen in a glovebox or using standard Schlenk procedures, unless otherwise stated. Solvents were dried using conventional procedures. Deuterated solvents were degassed and distilled from CaH_2. Unless otherwise stated, commercial reagents were used without further purification. Norbornene, 1,10-dibromodecane, 1,9-dibromononane, and 1,5-dibromopentane were dried over activated sieves and distilled. Norbornylmethylene bromide[45] and $\{Mo(NAr)(OR_{F6})_2[=CHC_5H_4]\}_2Fe$[41] were prepared according to the literature.

NMR spectra were recorded on a Varian INOVA 500 spectrometer. ^1H NMR chemical shifts are given in ppm vs residual protons in the deuterated solvents as follows: δ 7.27 $CDCl_3$, δ 7.16 C_6D_6, δ 2.5 $(CD_3)_2SO$. For calculation of all polymer compositions the relaxation time D1 was set to 15 s. Some GPC analyses (solvent = methylene chloride, 1 mL/min) were carried out on a system equipped with two Jordi-Gel DVB mixed bed columns (250 mm length × 10 mm inner diameter) in series. A Wyatt Technology mini Dawn light-scattering detector coupled with a Knauer differential refractometer was employed. PDI values for polymers on this system were obtained using d*n*/d*c* = 0.132 mL/g. Other GPC analyses (solvent = tetrahydrofuran, 1 mL/min) were carried out using a Waters GPC system equipped with 1 Styragel HT3 column (500−30 000 MW range), 1 Styragel HT4 column (5000−600 000 MW range), 1 Styragel HT5 column (50 000−4×10^6 MW range), a refractive index detector, and a UV detector (254 nm) was used for molecular weight measurement relative to polystyrene standards. All polymer samples were cast from a concentrated (∼10 wt %) toluene solution onto a Teflon coated sheet and then air-dried for ∼24 h. A TA Instruments Q1000 was used for differential scanning calorimetry (DSC); the heating and cooling rates were 5 °C min^{-1} in all cases. The optical micrographs were taken using a Zeiss Axioskop2 polarized light microscope with a Zeiss AxioCam HRc digital camera. The samples were heated using a Linkam THMS 600 hot stage at a rate of 5 °C min^{-1}. A TA Instruments Q800 was used for dynamic mechanical analysis (DMA). The heating rate was 3 °C min^{-1}, and oscillations of amplitude of 25 μm were applied to films in 0.02 MPa of tension at a frequency of 1 Hz. SAXS data were collected with a Siemens 2-D small-angle X-ray scattering detector. The X-rays were Cu Kα radiation with a wavelength 0.1542 nm, set at 40 kV and 0.66 mA. Silver behenate was used to calibrate the sample-to-detector distance with a first-order scattering vector of q of 1.076 nm^{-1} (with $q = (4\pi \sin \theta)/\lambda$ where 2θ is the scattering angle and λ is the wavelength).

Synthesis of 5-(6-Bromohexyl)bicyclo[2.2.1]hept-2-ene. This procedure was adapted from the literature.[46] Magnesium turnings (3.10 g, 0.128 mol) in 100 mL of THF were placed in a three-neck flask equipped with a condenser, nitrogen inlet, and addition funnel containing norbornylmethylene bromide (20 g, 0.106 mol). The norbornene was slowly added to the magnesium over an hour period, and the solution was refluxed and stirred overnight. The solution was cooled and transferred via a cannula into an addition funnel that was attached to a Schlenk flask charged with Li_2CuCl_4 (0.1 M in THF, 11 mL) and 1,5-dibromopentane (30 g, 0.130 mol). The reaction mixture was cooled to approximately −20 °C, and the Grignard solution was added slowly over 2 h. The reaction was slowly warmed to room temperature overnight. Diethyl ether (100 mL) was added to the solution, and it was washed with saturated NH_4Cl solution. The aqueous layer was extracted with ether; the organic layers were combined and then washed with brine. The volatile components were removed on the rotovap, and the residue was distilled under reduced pressure; yield of crude oil 10.96 g (41%, 0.043 mol). This fraction was purified by column chromatography on silica gel using hexanes (R_f = 0.53). A total of 6 g (22%) of clean product (colorless oil) was isolated from this first column. A second column was run on the remaining residues, and the yield from this was 3.86 g (14%; endo:exo = 80:20). ^1H NMR ($CDCl_3$) (all peaks reported are for this isomer unless otherwise stated): δ 6.10 (1H, m, *H*CCH_{endo}), δ 6.08 (1H, m, *H*CCH_{exo}), δ 6.02 (1H, m, HC*C*H_{exo}), δ 5.91 (1H, m, HC*C*H_{endo}), δ 3.42 (2H, m, $(CH_2)_5CH_2Br$), δ 2.78 (1H, s, CHCHC*H*CH_{2exo}), δ 2.75 (1H, s, CHCHC*H*CH_{2endo}), δ 2.50 (1H, s, 1H, s, CHCHC*H*CH_{2exo}), δ 1.97 (1H, m, $(CH_2)_6CH$), δ 1.8−1.1 (12H, m), δ 0.49 (1H, m, $(CH_2)_5$-CHC*H*H). $^{13}C\{^1H\}$ NMR ($CDCl_3$, major isomer only): δ 137.07, 132.53, 49.73, 45.55, 42.68, 38.87, 34.85, 34.21, 33.02, 32.58, 29.20, 28.63, 28.38.

Synthesis of 5-(10-Decahexyl)bicyclo[2.2.1]hept-2-ene. Prepared in a similar manner as described for 5-(6-bromohexyl)bicyclo-[2.2.1]hept-2-ene. A total of 6.2 g (37%, 0.020 mol) of clean product (colorless oil) was isolated from the column; endo:exo = 80:20. ^1H NMR ($CDCl_3$) (all peaks reported are for this isomer unless otherwise stated): δ 6.10 (1H, m, *H*CCH_{endo}), δ 6.08 (1H, m, *H*CCH_{exo}), δ 6.02 (1H, m, HC*C*H_{exo}), δ 5.91 (1H, m, HC*C*H_{endo}), δ 3.42 (2H, m, $(CH_2)_5CH_2Br$), δ 2.78 (1H, s, CHCHC*H*CH_{2exo}), δ 2.75 (1H, s, CHCHC*H*CH_{2endo}), δ 2.74 (1H, s, CHCHC*H*CH_{2endo}), δ 2.50 (1H, s, 1H, s, CHCHC*H*CH_{2exo}), δ 1.97 (1H, m, $(CH_2)_6CH$), δ 1.8−1.1 (21H, m), δ 0.48 (1H, m, $(CH_2)_5CHCHH$). $^{13}C\{^1H\}$ NMR ($CDCl_3$, major isomer only): δ 137.04, 132.65, 49.75, 45.59, 42.71, 38.94, 35.01, 34.31, 33.05, 32.63, 30.10, 29.84, 29.75, 29.65, 28.99, 28.67, 28.39.

Synthesis of 2-(10-Bromodecyl)bicyclo[2.2.1]hepta-2,5-diene. This procedure was adapted from the literature.[47] A three-neck flask equipped with a nitrogen inlet was charged with potassium *tert*-butoxide (3.9 g, 0.035 mol) and norbornadiene (5 mL, 0.046 mol) in THF (100 mL). The solution was cooled to −78 °C, and *n*-butyllithium (13.6 mL, 2.5 M, 0.035 mol) was added dropwise over a period of 1 h, while keeping the temperature below −65 °C. The solution was stirred at −65 °C for 30 min and then at −40 °C for 30 min. It was then cooled to −78 °C and transferred via a cannula over a period of 1 h to a second flask charged with 1,10-dibromodecane (13 mL, 0.058 mol) in THF (100 mL), which was cooled to −65 °C. After the addition was complete, the reaction

was stirred at −40 °C for 2 h and then at 0 °C for 2 h. At this time, the reaction was quenched with saturated NH_4Cl (50 mL) and H_2O (50 mL). The reaction was extracted with ether (3 × 200 mL). The organic layers were combined and washed with water and brine. The organic layer was dried with Mg_2SO_4, and the volatile components were removed by rotovap. The residue was distilled under reduced pressure. The first fraction that was distilled was mostly 1,10-dibromodecane. The second fraction (oil: 200 °C; head: 130 °C; pressure: 300 mTorr) was clean 2-(10-bromodecyl)-bicyclo[2.2.1]hepta-2,5-diene (2.8 g, 26%, 0.0090 mol). ^{1}H NMR ($CDCl_3$): δ 6.76 (2H, m, *H*CC*H*), δ 6.12 (1H, m, C*H*), δ 3.50 (1H, s, CHCHC*H*CH_2), δ 3.42 (2H, t, C*H*$_2$Br), δ 3.28 (1H, s, CHCHC*H*CH_2), δ 2.18 (2H, m, CHCC*H*$_2$), δ 1.96 (2H, s, C*H*$_2$-norbornadiene), δ 1.86 (2H, m, C*H*$_2$$CH_2$O), δ 1.41−1.25 (14H, m, CH_2(C*H*$_2$)$_7$$CH_2$$CH_2$O). ^{13}C{^{1}H} NMR ($CDCl_3$): δ 159.24, 144.01, 142.59, 133.27, 73.63, 53.66, 50.17, 34.27, 33.01, 31.71, 29.65, 29.62, 29.60, 29.53, 28.94, 28.36, 27.39. HRMS (ESI) Calcd for $C_{17}H_{27}Br$ [M]: 310.1291. Found: 310.1296.

Synthesis of NB6. A three-neck flask equipped with a condenser was charged with KOH (1.5 g), ethanol (195 mL), water (9.7 mL), a few crystals of KI, and 4′-hydroxybiphenyl-4-carboxylic acid (2.5 g, 0.012 mol). The solution was heated to reflux, and 5-(6-bromohexyl)bicyclo[2.2.1]hept-2-ene (6 g, 0.023 mol) was added. The solution was allowed to reflux overnight, at which time a solution of 10% KOH in 70% ethanol was added. The solution became yellow in color and was refluxed for an additional 3 h. The compound was allowed to cool at which time a dilute solution of HCl was added in order to hydrolyze the secondary ester product. The solid formed was collected and washed with ethanol and water. The white product was insoluble in most organics; yield 4.2 g (92%, 0.011 mol). The powder was triturated with pentane and dried in vacuo overnight. The compound isolated was then further reacted to yield **NB6wBPP4**, thereby confirming the identity of the isolated product.

Synthesis of NB10. Prepared in a similar manner as described for **NB6**; yield 3.4 g (79%, 0.0041 mol). ^{1}H NMR (all peaks reported are for the major isomer (endo:exo = 80:20), unless otherwise stated): δ 12.92 (1H, s, COO*H*), δ 7.97 (2H, d, aromatic C*H*), δ 7.54 (2H, d, aromatic C*H*), δ 7.67 (2H, d, aromatic C*H*), δ 7.03 (2H, d, aromatic C*H*), δ 6.11 (1H, m, *H*CCH$_{endo}$), δ 6.08 (1H, m, *H*CCH$_{exo}$), δ 6.02 (1H, m, *H*CCH$_{exo}$), δ 5.91 (1H, m, HCC*H*$_{endo}$), δ 4.01 (2H, m, $(CH_2)_9$C*H*$_2$O), δ 2.72 (1H, s, CHCHC*H*CH_{2exo} and $_{endo}$), δ 1.93, 1.79, (both 1H, m), δ 1.73, 1.41 (both 2H, m), δ 1.31−10.98 (17 H, m), δ 0.41 (1H, m, C*H*HCH$(CH_2)_{10}$). HRMS (ESI) Calcd for $C_{30}H_{38}O_3$ [M+]: 446.2815. Found: 446.2819.

Synthesis of NBD10. Prepared in a similar manner as described for **NB6**; yield 1.8 g (84%). ^{1}H NMR $(CD_3)_2SO$): δ 12.92 (1H, s, COO*H*), δ 7.98 (2H, d, aromatic C*H*), δ 7.78 (2H, d, aromatic C*H*), δ 7.67 (2H, d, aromatic C*H*), δ 7.03 (2H, d, aromatic C*H*), δ 6.73 (2H, m, *H*CC*H*), δ 6.10 (1H, m, C*H*), δ 4.00 (2H, t, OC*H*$_2$), δ 3.45 (1H, s, CHCHC*H*CH_2), δ 3.26 (1H, s, CHCHC*H*CH_2), δ 2.13 (2H, m), δ 1.86 (2H, m), δ 1.72 (2H, m), δ 1.41−1.25 (14H, m). HRMS (ESI$^-$) Calcd for $C_{30}H_{36}O_3$ [M−H]: 443.2581. Found: 443.2582.

Synthesis of NB6wBPP4. To a round-bottom flask was added **NB6** (3.7 g, 9.5 mmol), (dimethylamino)pyridine (0.12 g, 0.95 mmol), (+)-butyl-2-(4-hydroxyphenoxy)propanoate (2.25 g, 9.5 mmol), and dry methylene chloride (100 mL) under a N_2 atmosphere. The solution was cooled to 0 °C, dicyclohexylcarbodiimide (4.9 g, 23.7 mmol) in methylene chloride was added, and the reaction was allowed to stir overnight and slowly warm to room temperature. The reaction solution was filtered, and the volatile components were removed by rotovap. The compound was purified by column chromatography on silica gel using 1:9 ethyl acetate:hexanes. The appropriate fraction (R_f = 0.42) was dried with Mg_2SO_4, and the volatile components were removed by rotovap. The white powder was dried in vacuo, and 3.0 g (52%, 0.0049 mol) was isolated. ^{1}H NMR (C_6D_6) (all peaks reported are for the major isomer (endo:exo = 80:20), unless otherwise stated): δ 8.31 (2H, d, aromatic C*H*), δ 7.45 (2H, d, aromatic C*H*), δ 7.37 (2H, d, aromatic C*H*), δ 7.05 (2H, d, aromatic C*H*), δ 6.91 (2H, d, aromatic C*H*), δ 6.86 (2H, d, aromatic C*H*), δ 6.11 (1H, m, *H*CCH$_{endo}$), δ 6.04 (1H, m, *H*CCH$_{exo}$), δ 5.95 (1H, m, HCC*H*$_{endo}$), δ 4.52 (1H, q, C*H*CH_3), δ 3.93 (2H, m, $(CH_2)_5$C*H*$_2$O), δ 3.71 (3H, m, OC*H*$_2$$CH_2$-$CH_2CH_3$), δ 2.73 (1H, s, CHCHC*H*CH_{2exo} and $_{endo}$), δ 2.69 (1H, s, CHCHC*H*CH_{2endo}), δ 2.48 (1H, s, CHCHC*H*CH_{2exo}), δ 1.93, 1.78, 1.52, (all 1H, m), δ 1.68 (2H, m), δ 1.45 (3H, d, CHC*H*$_3$), δ 1.41−1.00 (13 H, m), δ 0.73 (t, 3H, $CH_3(CH_2)_3O$), δ 0.54 (1H, m, C*H*HCH$(CH_2)_5$). ^{13}C{^{1}H} NMR (C_6D_6, major isomer only): δ 172.08, 165.46, 160.43, 156.33, 154.06, 146.40, 146.08, 137.55, 132.97, 131.40, 129.1, 128.68, 127.25, 123.47, 116.35, 115.58, 73.68, 68.41, 65.17, 50.32, 46.20, 43.32, 39.51, 35.50, 33.15, 31.10, 30.41, 30.01, 29.38, 26.80, 19.52, 18.97, 14.03. HRMS (ESI) Calcd for $C_{39}H_{46}O_6$ [M + Na]: 633.3186. Found: 633.3164.

Synthesis of NB10wBPP4. Prepared in a similar manner as described for **NB6wBPP4**; yield 1.9 g (43%, 0.0029 mol). ^{1}H NMR {$CDCl_3$) (all peaks reported are for the major isomer (endo:exo = 80:20), unless otherwise stated): δ 8.22 (2H, d, aromatic C*H*), δ 7.69 (2H, d, aromatic C*H*), δ 7.60 (2H, d, aromatic C*H*), δ 7.14 (2H, d, aromatic C*H*), δ 7.01 (2H, d, aromatic C*H*), δ 6.93 (2H, d, aromatic C*H*), δ 6.11 (1H, m, *H*CCH$_{endo}$), δ 6.08 (1H, m, *H*CCH$_{exo}$), δ 6.01 (1H, m, *H*CCH$_{exo}$), δ 5.91 (1H, m, HCC*H*$_{endo}$), δ 4.75 (1H, q, C*H*CH_3), δ 4.18 (2H, m, $(CH_2)_9$C*H*$_2$O), δ 4.03 (3H, m, OC*H*$_2$-$CH_2CH_2CH_3$), δ 2.76 (1H, s, CHCHC*H*CH_{2exo} and $_{endo}$), δ 2.74 (1H, s, CHCHC*H*CH_{2exo}), δ 2.51 (1H, s, CHCHC*H*CH_{2endo}), δ 2.0−1.5 (129 H, m), δ 0.92 (t, 3H, $CH_3(CH_2)_3O$), δ 0.49 (1H, m, C*H*HCH$(CH_2)_5$). ^{13}C {^{1}H} NMR (C_6D_6, major isomer only): δ 172.06, 165.45, 160.41, 156.32, 146.41, 146.07, 137.51, 132.97, 132.70, 131.38, 129.12, 127.25, 123.45, 116.34, 115.56, 73.38, 68.39, 65.16, 50.31, 46.22, 43.32, 39.59, 39.55, 35.63, 33.16, 31.09, 30.77, 30.51, 30.43, 30.40, 30.18, 29.99, 29.52, 26.80, 19.50, 18.95, 14.01. HRMS (ESI) Calcd for $C_{43}H_{54}O_6$ [M + Na]: 689.3813. Found: 689.3834

Synthesis of NBD10wBPP4. Prepared in a similar manner as described for **NB6wBPP4**; yield 1.0 g (44%, 0.0015 mol). ^{1}H NMR ($CDCl_3$): δ 8.22 (2H, d, aromatic C*H*), δ 7.69 (2H, d, aromatic C*H*), δ 7.60 (2H, d, aromatic C*H*), δ 7.14 (2H, d, aromatic C*H*), δ 7.02 (2H, d, aromatic C*H*), δ 6.93 (2H, d, aromatic C*H*), δ 6.76 (2H, m, *H*CC*H*), δ 6.12 (1H, s, CC*H*), δ 4.75 (1H, q, CH_3C*H*), δ 4.18 (2H, m, OC*H*$_2$$CH_2CH_2CH_3$), δ 3.56 (2H, m OC*H*$_2$$(CH_2)_9$), δ 3.50 (1H, m, CHCHC*H*CH_2), δ 3.28 (1H, m, CHCHC*H*CH_2), δ 2.18, 1.96 (both 2H, m), δ 1.64 (3H, d, C*H*$_3$CH), δ 1.63−1.2 (18 H, m), δ 0.92 (3H, t, C*H*$_3$$CH_2CH_2CH_2O$). ^{13}C {^{1}H} NMR ($CDCl_3$): δ 172.35, 165.48, 159.71, 159.22, 155.46, 146.06, 145.28, 143.98, 142.56, 133.26, 132.09, 130.83, 128.53, 127.64, 126.71, 122.75, 116.02, 115.12, 73.61, 73.33, 68.28, 65.33, 53.65, 50.15, 31.70, 30.68, 29.72, 29.70, 29.64, 29.55, 29.54, 29.41, 27.39, 26.21, 19.14, 18.80, 13.81. HRMS (ESI) Calcd for $C_{43}H_{52}O_6$ [M + Na]: 687.3656. Found: 687.3664.

Example of Homopolymerization: Synthesis of Poly-(NB6wBPP4)$_{100}$. {Mo(NAr)(OR$_{F6}$)$_2$[=CHC$_5$H$_4$]}$_2$Fe (5.0 mg, 0.0033 mmol) and **NB6wBPP4** (203 mg, 0.33 mmol, 100 equiv) were weighed into separate vials, and toluene was added to each. The monomer solution was added to the catalyst and allowed to rapidly stir for 1 h. At this time, two drops of benzaldehyde were added, and the solution was allowed to stir for another hour. The solution was then brought out of the box, added to methanol (100 mL), and allowed to sit overnight. The solution was filtered through a pad of Celite on which the precipitate collected. The precipitate was then washed through with tetrahydrofuran, and the volatile components were removed to yield poly(**NB6wBPP4**)$_{100}$; yield 169 mg (83%).

Example of Triblock Copolymerization: Synthesis of Poly-(MTD)$_{50}$(NB6wBPP4)$_{200}$(MTD)$_{50}$. {Mo(NAr)(OR$_{F6}$)$_2$ [=CHC$_5$H$_4$]}$_2$-Fe (4.5 mg, 0.00299 mmol) and **NB6wBPP4** (365 mg, 0.598 mmol, 200 equiv) were weighed into separate vials, and toluene was added to each. The monomer solution was added to the catalyst and allowed to rapidly stir for 1 h. A solution of MTD (52 mg, 0.299 mmol, 100 equiv) in toluene was added, and the solution was stirred for another hour. At this time, a couple drops of benzaldehyde were added, and the solution was allowed to stir for another hour. The solution was then brought out of the box, added to methanol (100

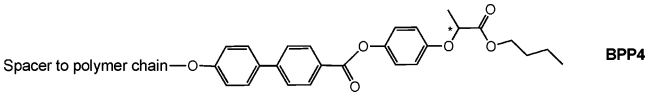

Figure 1. BPP4 mesogen.

Scheme 1

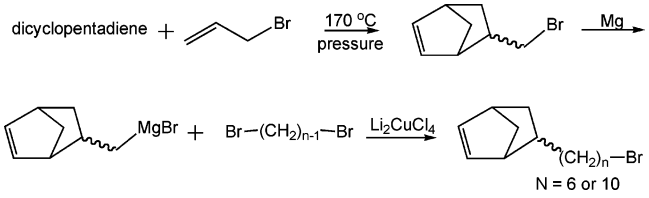

Scheme 2

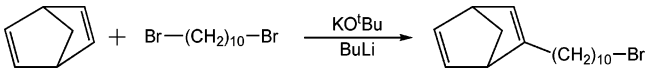

mL), and allowed to sit overnight. The solution was filtered through a pad of Celite on which the precipitate collected. The precipitate was then washed through with tetrahydrofuran, and the volatile components were removed to yield poly(MTD)$_{50}$(**NB6wBPP4**)$_{200}$-(MTD)$_{50}$; yield 462 mg (109%). The greater than 100% yield is ascribed to the presence of residual solvent in the polymer.

Results and Discussion

Synthesis of Monomers. We chose to examine a series of three monomers that contain the liquid crystal mesogen, BPP4 (Figure 1), as it has been found to exhibit a smectic C* phase in other systems.[44,48] One set of monomers has the LC mesogen attached to norbornene by a 6- or 10-carbon spacer ((*R*)-4′-(5-bicyclo[2.2.1]hept-5-en-2-yl-pentyloxy)-BPP4, **NB6wBPP4**, and (*R*)-4′-(10-bicyclo[2.2.1]hept-5-en-2-yl-decyloxy)-BPP4, **NB10wBPP4**, respectively). Therefore, we can compare the effects of an increase in the length of the carbon spacer in the triblock copolymers synthesized. The third monomer contains the LC mesogen attached to norbornadiene with a 10-carbon spacer ((*R*)-4′-(10-bicyclo[2.2.1]hepta-2,5-dien-2-yl-decyloxy)-BPP4, **NBD10wBPP4**). We might expect a polymer prepared from **NBD10wBPP4** to have a more rigid backbone than a polymer prepared from **NB10wBPP4**.

The halogen-functionalized norbornenes required for the **NB*n*wBPP4** monomers (exo:endo = 20:80, n = 6 or 10) were synthesized according to Scheme 1 through reaction of the appropriate *n*-bromo-functionalized compound through copper-catalyzed Grignard coupling with bromomethylnorbornene. The corresponding halogen-functionalized norbornadiene required for **NBD10wBPP4** was synthesized according to Scheme 2 by deprotonation of norbornadiene with Schlosser's base followed by reaction with 1,10-dibromodecane. These bromide-functionalized compounds could then be treated with 4′-hydroxy-4-biphenylcarboxylic acid to form one-half of the corresponding monomers, **NB6**, **NB10**, and **NBD10**. Further coupling with (+)-butyl-2-(4-hydroxyphenoxy)propanoate yielded the desired monomers **NB6wBPP4**, **NB10wBPP4**, and **NBD10wBPP4**, respectively, as shown in Scheme 3.

Polymerization of Monomers. Monomers **NB*n*wBPP4** (n = 6 or 10) and **NBD10wBPP4** were polymerized in quantitative yields in toluene using the bimetallic initiator, {Mo(NAr)-(OR$_{F6}$)$_2$[=CHC$_5$H$_4$]}$_2$Fe (Ar = 2,6-diisopropylphenyl, OR$_{F6}$ = OCMe(CF$_3$)$_2$) (Scheme 4). The molecular weight of the polymers was varied by controlling the molar ratio of monomer to initiator ([M]/[I]). For the synthesis of a homopolymer, benzaldehyde was added after 1 h in order to quench the polymerization. For the synthesis of a triblock copolymer, the

Scheme 3

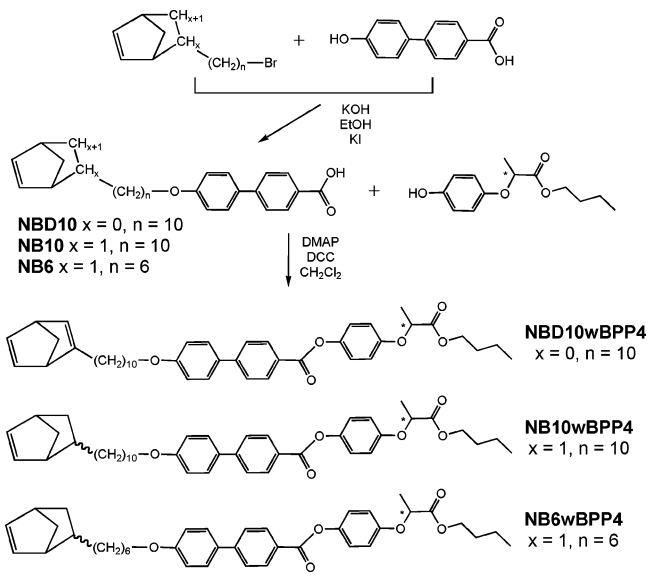

desired amount of methyltetracyclododecene (MTD) was added to the stirred mixture after 1 h. After an additional hour had elapsed, benzaldehyde was added to quench the polymerization. In all cases, the polymers were isolated by precipitation from methanol.

A series of homopolymers of **NB6wBPP4** were synthesized in order to demonstrate that the polymerization is living. The isolated yields of the polymers were all greater than 90%. As shown in Figure 2, a linear relationship is obtained by plotting the number-average molecular weight values (M_n vs polystyrene) of poly(**NB6wBPP4**) as a function of [M]/[I]. The results are summarized in Table 1. The linear relationship observed and the low polydispersities are consistent with living polymerization under the conditions employed. The experimental M_n values cannot be directly compared to the expected M_n values as the GPC system used was calibrated using polystyrene standards. The bimetallic initiator was previously shown to give experimental M_n values close to the expected M_n value (within 4%) as determined by MALDI−TOF MS when using norbornene-based monomers.[41]

Homopolymers (100-mers) of the other two monomers (**NB10wBPP4** and **NBD10wBPP4**) were synthesized, as well as triblock copolymers of all monomers, where methyltetracyclododecene (MTD) was the outer hard block (50 equiv per side) and the inner block was a liquid crystal functionalized monomer (200 equiv). The results of these polymerizations are summarized in Table 2, and the gel permeation chromatographs (GPCs) of the polymers are shown in Figure 3. Polydispersities (PDI) are less than 1.13 for the homopolymers and 1.31 for the triblock copolymers. Isolated yields were all greater than 90%.

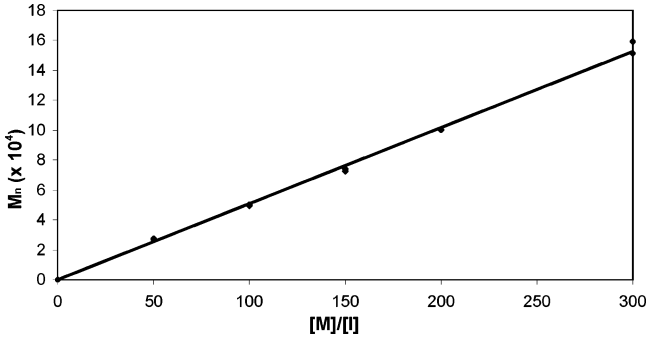

Figure 2. Graph of [M]/[I] vs M_n for homopolymers of poly(**NB6wBPP4**).

Scheme 4

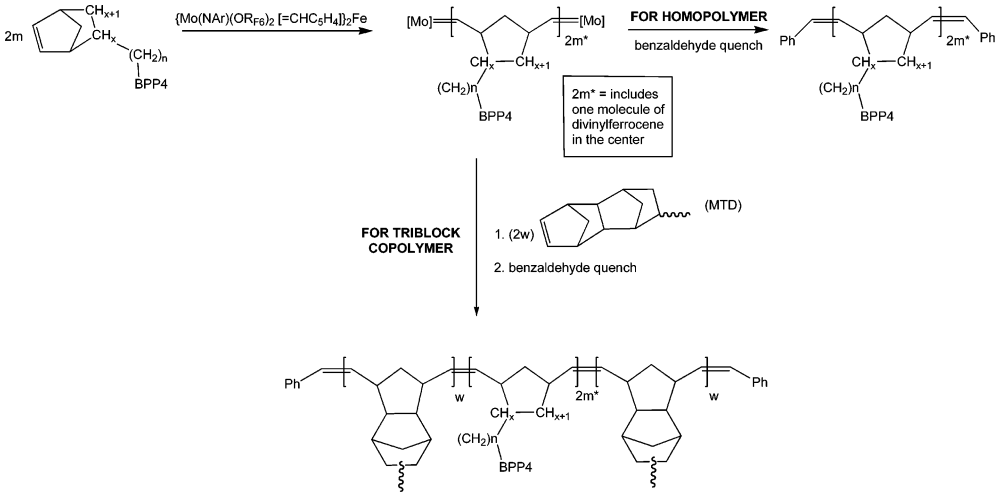

Table 1. Summary of GPC Data for Poly(NB6wBPP4) Homopolymers

equiv	expected M_n ($\times 10^4$)	actual M_n ($\times 10^4$)[a]	polydispersity
50	3.1	2.7, 2.7	1.18, 1.18
100	6.1	4.9, 5.0	1.10, 1.11
150	9.2	7.2, 7.4	1.09, 1.11
200	12.2	10.0, 10.0	1.12, 1.13
300	18.3	15.1, 15.9	1.15, 1.15

[a] M_n versus polystyrene standards. Samples run in tetrahydrofuran.

Proton NMR resonances in the olefinic range were quite broad, indicating a lack of stereoregularity of the main chain. The ^{1}H NMR spectra of the triblock copolymers were virtual superpositions of the two homopolymers, as shown in Figure 4. The ratio of the integration of the resonances in the olefinic region was used to approximate the ratio of LC functionalized monomer to MTD. These values are given in Table 2 and are close to the expected value of 0.5. The low polydispersities, correct ratio of monomers, and quantitative yields are consistent with a living system. Although the polymers are not indefinitely stable toward oxidation, the same set of polymers were used for all further characterizations over a period of 8 months.

Thermal Characterization of Polymers. The homopolymers and triblock copolymers were analyzed by differential scanning calorimetry (DSC) to determine the glass transition temperatures (T_g) of the central blocks with the attached mesogens. All values are reported in Table 3, and DSC traces of the second heating and first cooling of the triblock copolymers are shown in Figure 5. There was no notable difference observed when comparing the three monomers with increased length of the carbon spacer (**NB6wBPP4** vs **NB10wBPP4**) or with increased rigidity of the backbone structure (**NB10wBPP4** vs **NBD10wBPP4**). The T_g of the inner blocks of the respective triblock copolymers corresponded to the T_g of the LC homopolymers at ~20 °C, suggesting that the blocks are well phase segregated. However, the T_g of the MTD blocks was not observed in any of the three triblock copolymers. In DSC scans of a homopolymer of MTD, we observed a transition at ~220 °C. In the triblock copolymers, the weight percentage of MTD is too small for its glass transition to be observed. A second possible explanation is that there may be some phase mixing in the continuous phase of the system.

Phase transitions in the liquid crystalline sections of the monomers, homopolymers, and triblock copolymers were explored via DSC as reported in Table 3. The DSC transitions at low temperatures indicate the crystallization of the monomers, which behave as classical low molar mass liquid crystals. The smectic to isotropic transitions occur in these compounds at ~85 °C for all three monomers.

Side chain crystallization is not observed in the homopolymers over the temperature range of the DSC scans; as is observed with the majority of LC polymers, the material exists as a glass at low temperature and transitions directly into the LC phase at the T_g. The smectic-to-isotropic transition is observed at higher temperatures in the homopolymer than in low molar mass monomer, and there is also a broadening of the transitions that occurs on attachment to the polymer backbone. In general, it is expected that certain LC phases are stabilized when mesogens are attached to polymer backbones; this trend has been reported in other systems.[10,23,30] The smectic-to-isotropic transitions are elevated near 150 °C for all three homopolymers.

In DSC scans of the triblock copolymers, there are slight increases in the final smectic-to-isotropic phase transitions by a few degrees for the triblock copolymers containing **NB6wBPP4** and **NBD10wBPP4**. This suggests that the presence of the MTD block interface stabilizes the liquid crystalline phases. However, there is a slight decrease in the final smectic-to-isotropic phase transition for the triblock copolymer containing **NB10wBPP4**, suggesting a destabilization of the liquid crystalline phases. When analyzing the DSC scans for all three triblock copolymers, two transitions occur near the LC clearing point. In the triblock copolymer containing **NB6wBPP4**, however, the temperatures of the two transitions are so close that the peaks merge into one broad transition. The first of the two transitions is likely to be a smectic C* to A transition, whereas the second transition is the clearing point.

Further confirmation of the liquid crystal clearing points for the monomers, homopolymers, and triblock copolymers was established through polarized optical microscopy (POM). Birefringence for all samples was observed for the smectic liquid crystal phases, which disappeared as the temperature of the sample was increased above the liquid crystal clearing points. The POM data were in good agreement with the DSC data.

Small-angle X-ray scattering (SAXS) was performed on the triblock copolymers in order to investigate the morphology of the block copolymer and the liquid crystalline mesophases. All three samples exhibited a scattering peak on the order of 30−40 nm, which indicates phase segregation (Figure 6). However, higher order peaks are not observed, which suggests that there is no long-range order. The high T_g of the MTD blocks could provide kinetic limitations for achieving well-ordered systems. The triblock copolymer with the **NB6wBPP4** block has a first-

Table 2. Summary of Polymerization Data for Homopolymers and Triblock Copolymers

polymer	M_n ($\times 10^4$)[a]	PDI	yield	expected A:B[b]	actual A:B[c]
(**NBD10wBPP4**)$_{100}$	7.8	<1.05	96		
(MTD)$_{50}$(**NBD10wBPP4**)$_{200}$(MTD)$_{50}$	14.9	1.05	94	0.5	0.48
(**NB10wBPP4**)$_{100}$	6.88	1.13	90		
(MTD)$_{50}$(**NB10wBPP4**)$_{200}$(MTD)$_{50}$	11.7	1.31	92	0.5	0.50
(**NB6wBPP4**)$_{100}$	6.95	1.07	95		
(MTD)$_{50}$(**NB6wBPP4**)$_{200}$(MTD)$_{50}$	18.0	1.22	95	0.5	0.48

[a] M_n versus polystyrene standards. Samples run in dichloromethane. [b] Ratio of monomer B vs monomer A according to added [M]/[I] ratios. [c] Ratio of monomer B vs monomer A according to ^{1}H NMR.

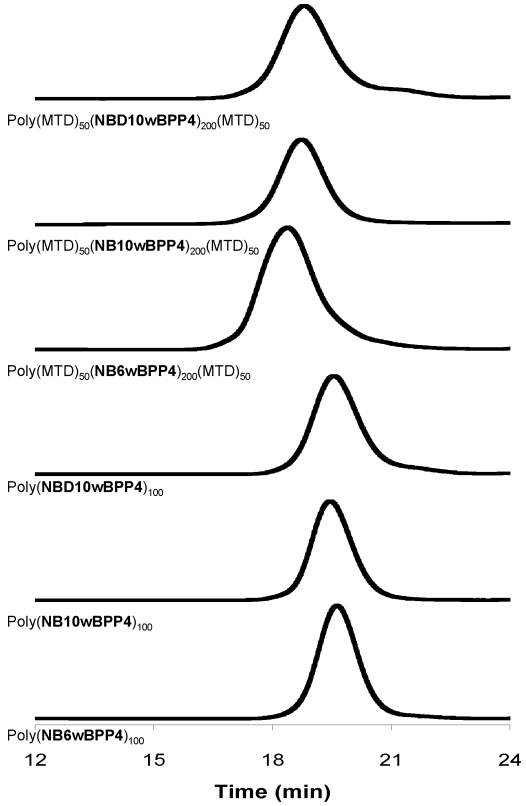

Figure 3. GPC traces of homo- and triblock copolymers.

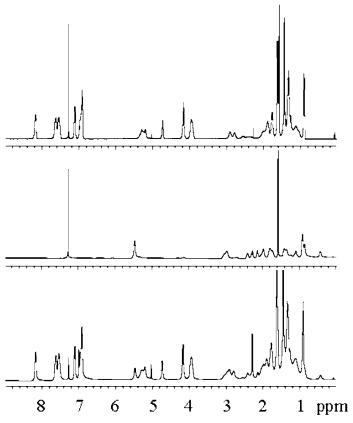

Figure 4. ^{1}H NMR of poly(**NB6wBPP4**)$_{100}$ (top), poly(MTD)$_{100}$ (middle), and poly(MTD)$_{50}$(**NB6wBPP4**)$_{200}$(MTD)$_{50}$ (bottom).

order scattering peak at 2.9 nm, indicating the presence of smectic monolayers. Considering the calculated molecular length of the mesogen unit attached to the backbone (3.5 nm[49]), it was concluded that triblock copolymers of **NB6wBPP4** form a smectic C* phase with a mesogen tilt angle of ~34° related to the layer normal.

The triblock copolymers containing **NB10wBPP4** and **NBD10wBPP4** have first-order scattering peaks at room temperature of 5.9 nm, suggesting the presence of smectic C* bilayers. However, when the former was heated to 100 °C, a scattering peak at 3.8 nm was observed, which indicated that a phase transition has occurred from the smectic C* bilayer to a monolayer. Across a broad range of intermediate temperatures, scattering for both layer spacings is observed, indicating that the two phases coexist. The tilt angles for the smectic C* phases are calculated to be ~42° and ~18° for the bilayer and the monolayer, respectively, when using a calculated molecular length of 4.0 nm.[49] However, it is possible that the mesogens are interpenetrated between bilayers, and therefore the given calculated tilt angle may be greater than the actual value. A similar bilayer-to-monolayer transition was observed for the triblock copolymer containing the **NBD10wBPP4** mesogen. It is not surprising that the transition from bilayers to monolayers was not observed in DSC and POM for these two triblock copolymers, as the transition occurs over a wide temperature range, with the two phases coexisting. In addition, the textures of liquid crystalline polymers in POM had very small domain sizes, inhibiting the ability to observe smectic-to-smectic transitions. The SAXS data affirmed that the two transitions observed near the LC clearing point are smectic C* to smectic A transitions followed by smectic A to isotropic transitions.

Dynamic mechanical analysis (DMA) confirmed the T_g of the LC polymer center block and also revealed the presence of an elastic plateau above the T_g of the LC center block in all of the triblock copolymers. The triblocks containing **NB6wBPP4** displayed an elastic plateau above the T_g of the LC center block until the onset of the smectic-to-isotropic transition, where the sample failed (Figure 7). However, in the triblock containing **NB10wBPP4**, the elastic plateau is interrupted by a transition near 70 °C, which is correlated with the smectic C* bilayer-to-monolayer transition (Figure 8). A similar DMA was also observed for the **NBD10wBPP4**-containing triblock copolymer, also confirming the bilayer-to-monolayer transition.

The elastomeric nature of the system is revealed by the presence of the elastic plateau in the DMA traces and indicates that these materials show potential for use as TPLCE actuators or other smart materials. In future studies, we will focus on systems with a lower T_g for both the inner and outer blocks. The T_g of the outer blocks will be optimized to ease the processability of the polymer as well as allow the system to achieve long-range ordering, while still providing enough rigidity to act as physical cross-links. The lower T_g of the inner block will enable the system to act as an elastomer at room temperature.

Conclusions

Liquid crystal functionalized monomers, **NB6wBPP4**, **NB10wBPP4**, and **NBDw10BPP4**, were synthesized and then polymerized by ring-opening metathesis polymerization in a living manner using the bimetallic molybdenum initiator, {Mo(NAr)(OR$_{F6}$)$_2$[=CHC$_5$H$_4$]}$_2$Fe. A series of triblock copolymers were synthesized, where the outer block was MTD. The liquid

Table 3. Summary of Thermal Data for Monomers, Homopolymers, and Triblock Copolymers

	monomer		homopolymers		triblock copolymers	
	heating	cooling	heating	cooling	heating	cooling
NBD10wBPP4	K 56 S_1 81 I	I 79 S_1 19 K	G_{LC} 20 S_C* 138−149 S_A 150 I	I 148 S_A 147−138 S_C* 20 G_{LC}	G_{LC} 20 S_C* 140−151 S_A 152 I	I 148 S_A 147−133 S_C* 20 G_{LC}
NB10wBPP4	K 68 S_1 88 I	I 86 S_1 42−33 K	G_{LC} 20 S_C* 138 S_A 161 I	I 158 S_A 128 S_C* 20 G_{LC}	G_{LC} 20 S_C* 134−149 S_A 150 I	I 146 S_A145−133 S_C* 20 G_{LC}
NB6wBPP4	K 65 S_1 86 I	I 85 S_1 18 K	G_{LC} 20 S_C* S_A 118−144 I	I 131 S_A 125 S_C* 20 G_{LC}	G_{LC} 20 S_C* S_A 128−158 I	I 155−120 S_A S_C* 20 G_{LC}

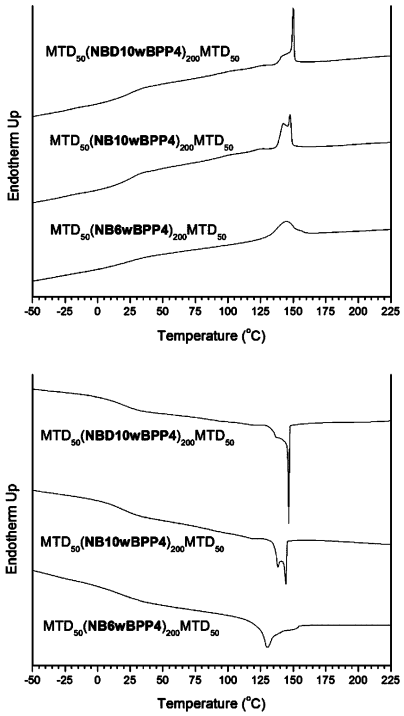

Figure 5. Second heating (top) and first cooling (bottom) DSC curves of $(MTD)_{50}(LC)_{200}(MTD)_{50}$ triblocks.

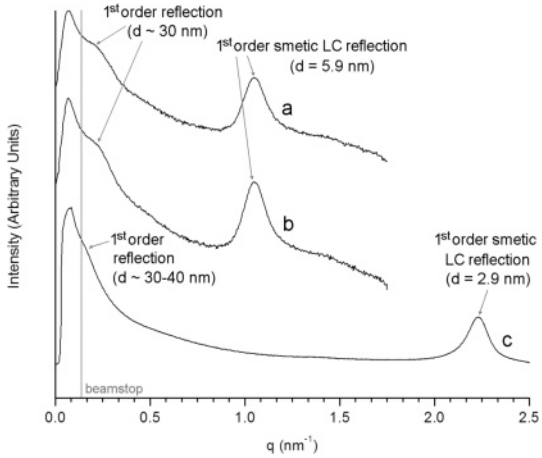

Figure 6. SAXS of (a) $(MTD)_{50}$(**NBD10wBPP4**)$_{200}(MTD)_{50}$, (b) $(MTD)_{50}$(**NB10wBPP4**)$_{200}(MTD)_{50}$, and (c) $(MTD)_{50}$(**NB6wBPP4**)$_{200}$-$(MTD)_{50}$.

crystalline polymer inner blocks exhibited glass transition temperatures around 20 °C, and the smectic-to-isotropic transitions were observed around 150 °C. SAXS studies showed that the triblock copolymers containing **NB6wBPP4** form a smectic C* monolayer, while those containing **NB10wBPP4** and **NBD10wBPP4** form smectic C* bilayers at room temperature. For the latter two triblock copolymers, a transition was observed at elevated temperatures, and two phases were observed, smectic C* bilayers and monolayers. In addition, phase segregation was

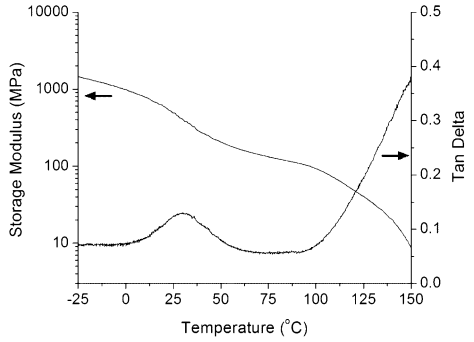

Figure 7. DMA of $(MTD)_{50}$(**NB6wBPP4**)$_{200}(MTD)_{50}$.

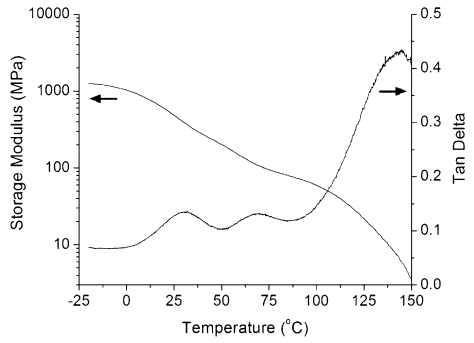

Figure 8. DMA of $(MTD)_{50}$(**NB10wBPP4**)$_{200}(MTD)_{50}$.

observed for the triblock copolymer systems, as indicated by the SAXS studies and correspondence of the glass transition temperature of the inner blocks to the homopolymer transitions. DMA analysis showed that the triblock copolymers exhibit elastic plateaus. The results of the studies of the triblock copolymers give evidence that with optimization ABA triblock copolymers synthesized via ROMP have the potential to act as TPLCEs, actuators, or shape-memory materials at elevated or at room temperature. Future studies will focus on developing systems that exhibit glass transition temperatures of the central block below operating temperatures (i.e., below room temperature) and increased phase separation and long-range order by altering the composition of the outer block.

Acknowledgment. This research was supported by the U.S. Army through the Institute for Soldier Nanotechnologies, under Contract DAAD-19-02-D-0002 with the U.S. Army Research Office. The contract does not necessarily reflect the position of the Government, and no official endorsement should be inferred. We thank NSERC of Canada for a postgraduate scholarship (PGS A) to A.G. We thank the DCIF staff at MIT for technical assistance.

References and Notes

(1) Grubbs, R. H.; Tumas, W. *Science* **1989**, *243*, 907−915.
(2) Odian, G. *Principles of Polymerization*; Wiley: New York, 1981.
(3) Rempp, R.; Merrill, E. W. *Polymer Synthesis*; Huthig and Wepf: New York, 1986.
(4) Webster, O. W. *Science* **1991**, *251*, 887−893.

(5) Schrock, R. R. *Acc. Chem. Res.* **1990**, *23*, 158−165.
(6) Bates, F. S.; Fredrickson, G. H. *Annu. Rev. Phys. Chem.* **1990**, *41*, 525−557.
(7) Noshay, A.; McGrath, J. E. *Block Copolymers*; Academic Press: New York, 1977.
(8) Nair, B. R.; Osbourne, M. A. R.; Hammond, P. T. *Macromolecules* **1998**, *31*, 8749−8756.
(9) Moment, A.; Miranda, R.; Hammond, P. T. *Macromol. Rapid Commun.* **1998**, *19*, 573−579.
(10) Moment, A.; Hammond, P. T. *Polymer* **2001**, *42*, 6945−6959.
(11) Terentjev, E. M.; Hotta, A.; Clarke, S. M.; Warner, M. *Philos. Trans. R. Soc. London Ser. A: Math. Phys. Eng. Sci.* **2003**, *361*, 653−663.
(12) Warner, M.; Bladon, P.; Terentjev, E. M. *J. Phys. II* **1994**, *4*, 93−102.
(13) Adams, J. M.; Warner, M. *Phys. Rev. E* **2005**, *72*, 011703.
(14) Clarke, S. M.; Tajbakhsh, A. R.; Terentjev, E. M.; Warner, M. *Phys. Rev. Lett.* **2001**, *86*, 4044−4047.
(15) Hiraoka, K.; Stein, P.; Finkelmann, H. *Macromol. Chem. Phys.* **2004**, *205*, 48−54.
(16) Lehmann, W.; Hartmann, L.; Kremer, F.; Stein, P.; Finkelmann, H.; Kruth, H.; Diele, S. *J. Appl. Phys.* **1999**, *86*, 1647−1652.
(17) Lehmann, W.; Skupin, H.; Tolksdorf, C.; Gebhard, E.; Zentel, R.; Kruger, P.; Losche, M.; Kremer, F. *Nature (London)* **2001**, *410*, 447−450.
(18) Naciri, J.; Srinivasan, A.; Jeon, H.; Nikolov, N.; Keller, P.; Ratna, B. R. *Macromolecules* **2003**, *36*, 8499−8505.
(19) Thomsen, D. L.; Keller, P.; Naciri, J.; Pink, R.; Jeon, H.; Shenoy, D.; Ratna, B. R. *Macromolecules* **2001**, *34*, 5868−5875.
(20) Clark, N. A.; Lagerwall, S. T. *Appl. Phys. Lett.* **1980**, *36*, 899−901.
(21) Anthamatten, M.; Zheng, W. Y.; Hammond, P. T. *Macromolecules* **1999**, *32*, 4838−4848.
(22) Fischer, H.; Poser, S.; Arnold, M.; Frank, W. *Macromolecules* **1994**, *27*, 7133−7138.
(23) Hamley, I. W.; Castelletto, V.; Lu, Z. B.; Imrie, C. T.; Itoh, T.; Al-Hussein, M. *Macromolecules* **2004**, *37*, 4798−4807.
(24) Hamley, I. W.; Davidson, P.; Gleeson, A. J. *Polymer* **1999**, *40*, 3599−3603.
(25) Hiraoka, K.; Uematsu, Y.; Stein, P.; Finkelmann, H. *Macromol. Chem. Phys.* **2002**, *203*, 2205−2210.
(26) Osuji, C.; Zhang, Y. M.; Mao, G. P.; Ober, C. K.; Thomas, E. L. *Macromolecules* **1999**, *32*, 7703−7706.
(27) Poser, S.; Fischer, H.; Arnold, M. *J. Polym. Sci., Part A* **1996**, *34*, 1733−1740.
(28) Sentenac, D.; Demirel, A. L.; Lub, J.; de Jeu, W. H. *Macromolecules* **1999**, *32*, 3235−3240.
(29) Yamada, M.; Itoh, T.; Hirao, A.; Nakahama, S.; Watanabe, J. *High Perform. Polym.* **1998**, *10*, 131−138.
(30) Zheng, W. Y.; Albalak, R. J.; Hammond, P. T. *Macromolecules* **1998**, *31*, 2686−2689.
(31) Pugh, C.; Schrock, R. R. *Macromolecules* **1992**, *25*, 6593−6604.
(32) Komiya, Z.; Pugh, C.; Schrock, R. R. *Macromolecules* **1992**, *25*, 3609−3616.
(33) Komiya, Z.; Pugh, C.; Schrock, R. R. *Macromolecules* **1992**, *25*, 6586−6592.
(34) Komiya, Z.; Schrock, R. R. *Macromolecules* **1993**, *26*, 1387−1392.
(35) Komiya, Z.; Schrock, R. R. *Macromolecules* **1993**, *26*, 1393−1401.
(36) Ungerank, M.; Winkler, B.; Stelzer, F. Side Chain Liquid Crystalline Polymers via ROMP. In *Metathesis Polymerization of Olefins and Polymerization of Alkynes*; Imamoglu, Y., Ed.; Kluwer Academic Publishers: Dordrecht, The Netherlands, 1998; pp 225−241.
(37) Trimmel, G.; Riegler, S.; Fuchs, G.; Slugovic, C.; Stelzer, F. *Liquid Crystalline Polymers by Metathesis Polymerization*; Springer: Dordrecht, The Netherlands, 2005; Vol. 176, pp 43−88.
(38) Pugh, C.; Kiste, A. L. *Prog. Polym. Sci.* **1997**, *22*, 601−691.
(39) Mayerschofer, M. G.; Nuyken, O.; Buchmeiser, M. R. *Macromolecules* **2006**, *39*, 2452−2459.
(40) Risse, W.; Wheeler, D. R.; Cannizzo, L. F.; Grubbs, R. H. *Macromolecules* **1989**, *22*, 3205−3210.
(41) Schrock, R. R.; Gabert, A. J.; Singh, R.; Hock, A. S. *Organometallics* **2005**, *24*, 5058−5066.
(42) Weck, M.; Schwab, P.; Grubbs, R. H. *Macromolecules* **1996**, *29*, 1789−1793.
(43) Wu, Z.; Grubbs, R. H. *Macromolecules* **1994**, *27*, 6700−6703.
(44) Svensson, M.; Helgee, B.; Skarp, K.; Andersson, G. *J. Mater. Chem.* **1998**, *8*, 353−362.
(45) Dolman, S. J.; Hultzsch, K. C.; Pezet, F.; Teng, X.; Hoveyda, A. H.; Schrock, R. R. *J. Am. Chem. Soc.* **2004**, *126*, 10945−10953.
(46) Stubbs, L. P.; Weck, M. *Chem.−Eur. J.* **2003**, *9*, 992−999.
(47) Yip, C.; Handerson, S.; Tranmer, G. K.; Tam, W. *J. Org. Chem.* **2001**, *66*, 276−286.
(48) Helgee, B.; Hjertberg, T.; Skarp, K.; Andersson, G.; Gouda, F. *Liq. Cryst.* **1995**, *18*, 871−878.
(49) The molecular lengths were calculated from minimized models of the molecules using Accelrys Materials Studio Molecular Modelling Software.

MA060243X